

# 20 THz-bandwidth continuous-wave fiber optical parametric amplifier operating at 1 $\mu\text{m}$ using a dispersion-stabilized photonic crystal fiber

A. Mussot,<sup>1,\*</sup> A. Kudlinski,<sup>1</sup> R. Habert,<sup>1</sup> I. Dahman,<sup>1</sup> G. Mélin,<sup>2</sup> L. Galkovsky,<sup>2</sup>  
A. Fleureau,<sup>2</sup> S. Lempereur,<sup>2</sup> L. Lago,<sup>3</sup> D. Bigourd,<sup>3</sup> T. Sylvestre,<sup>4</sup> M. W. Lee,<sup>4</sup> and  
E. Hugonnot<sup>3</sup>

<sup>1</sup> CNRS - Université Lille 1, PhLAM/IRCICA USR 3380/UMR 8523, F-59655 Villeneuve d'Ascq Cedex, France

<sup>2</sup> DRAKA, route de Nozay, 91460 Marcoussis, France

<sup>3</sup> Commissariat à l'Énergie Atomique et aux Énergies Alternatives, CESTA, 33116 Le Barp Cedex, France

<sup>4</sup> Institut FEMTO-ST, Département d'Optique, Université de Franche-Comté, CNRS UMR 6174, Besançon, France  
[mussot@phlam.univ-lille1.fr](mailto:mussot@phlam.univ-lille1.fr)

**Abstract:** We report the experimental demonstration of a continuous-wave all-fiber optical parametric amplifier in the 1  $\mu\text{m}$  band with a record bandwidth of more than 20 THz and a peak gain of almost 40 dB. This is achieved by using a photonic crystal fiber with a high figure of merit and strongly reduced longitudinal dispersion fluctuations. Due to their unique bandwidth and gain characteristics, fiber parametric amplifiers at 1  $\mu\text{m}$  provide an interesting alternative to solid-state or ytterbium-doped fiber amplifiers for ultrafast optical pulse and signal processing.

©2012 Optical Society of America

**OCIS codes:** (190.4380) Nonlinear optics, four-wave mixing; (190.4410) Nonlinear optics, parametric processes; (140.3280) Laser amplifiers.

---

## References and links

1. M. E. Marhic, *Fiber Optical Parametric Amplifiers, Oscillators and Related Devices*, 1<sup>st</sup> ed. (Cambridge University Press, 2007).
2. J. Hansryd, P. A. Andrekson, M. Westlund, Jie Li, and P. O. Hedekvist, "Fiber-based optical parametric amplifiers and their applications," *IEEE J. Sel. Top. Quantum Electron.* **8**(3), 506–520 (2002).
3. M. Jamshidifar, A. Vedadi, and M. E. Marhic, "Continuous-wave one-pump fiber optical parametric amplifier with 270 nm gain bandwidth," in 35th European Conference on Optical Communication (ECOC), p. 1–2 (2009).
4. T. Torounidis, P. A. Andrekson, and B.-E. Olsson, "Fiber-optical parametric amplifier with 70-dB gain," *IEEE Photon. Technol. Lett.* **18**(10), 1194–1196 (2006).
5. P. L. Voss, R. Tang, and P. Kumar, "Measurement of the photon statistics and the noise figure of a fiber-optic parametric amplifier," *Opt. Lett.* **28**(7), 549–551 (2003).
6. D. Bigourd, L. Lago, A. Mussot, A. Kudlinski, J.-F. Gleyze, and E. Hugonnot, "High-gain fiber, optical-parametric, chirped-pulse amplification of femtosecond pulses at 1  $\mu\text{m}$ ," *Opt. Lett.* **35**(20), 3480–3482 (2010).
7. D. Bigourd, L. Lago, A. Kudlinski, E. Hugonnot, and A. Mussot, "Dynamics of fiber optical parametric chirped pulse amplifiers," *J. Opt. Soc. Am. B* **28**(11), 2848–2854 (2011).
8. G. Melin, D. Labat, L. Galkovsky, A. Fleureau, S. Lempereur, A. Mussot, and A. Kudlinski, "Highly-nonlinear photonic crystal fibre with high figure of merit around 1  $\mu\text{m}$ ," *Electron. Lett.* **48**(4), 232–233 (2012).
9. M. W. Lee, T. Sylvestre, M. Delque, A. Kudlinski, A. Mussot, J.-F. Gleyze, A. Jolly, and H. Maillotte, "Demonstration of an all-fiber broadband optical parametric amplifier at 1  $\mu\text{m}$ ," *J. Lightwave Technol.* **28**(15), 2173–2178 (2010).
10. T. Sylvestre, A. Kudlinski, A. Mussot, J. F. Gleyze, A. Jolly, and H. Maillotte, "Parametric amplification and wavelength conversion in the 1040–1090 nm band by use of a photonic crystal fiber," *Appl. Phys. Lett.* **94**(11), 111104 (2009).
11. S. Randoux, N. Y. Joly, G. Mélin, A. Fleureau, L. Galkovsky, S. Lempereur, and P. Suret, "Grating-free Raman laser using highly nonlinear photonic crystal fiber," *Opt. Express* **15**(24), 16035–16043 (2007).
12. A. Kudlinski, G. Bouwmans, O. Vanvincq, Y. Quiquempois, A. Le Rouge, L. Bigot, G. Mélin, and A. Mussot, "White-light cw-pumped supercontinuum generation in highly GeO<sub>2</sub>-doped-core photonic crystal fibers," *Opt. Lett.* **34**(23), 3631–3633 (2009).
13. Y. P. Yatsenko, A. F. Kosolapov, A. E. Levchenko, S. L. Semjonov, and E. M. Dianov, "Broadband wavelength conversion in a germanosilicate-core photonic crystal fiber," *Opt. Lett.* **34**(17), 2581–2583 (2009).

14. B. Barviau, O. Vanvincq, A. Mussot, Y. Quiquempois, G. Melin, and A. Kudlinski, "Enhanced soliton self-frequency shift and CW supercontinuum generation in GeO<sub>2</sub>-doped core photonic crystal fibers," *J. Opt. Soc. Am. B* **28**(5), 1152–1160 (2011).
15. G. Mélin, S. Lempereur, A. Fleureau, L. Galkovsky, S. Richard, H. Maerten, E. Burov, and P. Nouchi, "Fabrication and characterization of germanium doped highly non-linear photonic crystal fibres," *Proceedings of SPIE*, **6990**, 699003, 699003-5 (2008).
16. A. Mussot, E. Lantz, A. Durecu-Legrand, C. Simonneau, D. Bayart, T. Sylvestre, and H. Maillotte, "Zero-dispersion wavelength mapping in short single-mode optical fibers using parametric amplification," *IEEE Photon. Technol. Lett.* **18**(1), 22–24 (2006).
17. M. Karlsson, "Four-wave mixing in fibers with randomly varying zero-dispersion wavelength," *J. Opt. Soc. Am. B* **15**(8), 2269–2275 (1998).
18. M. Farahmand and M. de Sterke, "Parametric amplification in presence of dispersion fluctuations," *Opt. Express* **12**(1), 136–142 (2004).
19. B. P.-P. Kuo, M. Hirano, and S. Radic, "Continuous-wave, short-wavelength infrared mixer using dispersion-stabilized highly-nonlinear fiber," *Opt. Express* **20**(16), 18422–18431 (2012).
20. B. P.-P. Kuo, J. M. Fini, L. Grüner-Nielsen, and S. Radic, "Dispersion-stabilized highly-nonlinear fiber for wideband parametric mixer synthesis," *Opt. Express* **20**(17), 18611–18619 (2012).
21. A. S. Y. Hsieh, G. K. L. Wong, S. G. Murdoch, S. Coen, F. Vanholsbeeck, R. Leonhardt, and J. D. Harvey, "Combined effect of Raman and parametric gain on single-pump parametric amplifiers," *Opt. Express* **15**(13), 8104–8114 (2007).
22. Y. Deng, C. Yu, J. Yuan, X. Sang, and W. Li, "Raman-induced limitation of gain flatness in broadband fiber-optical parametric amplifier," *Opt. Eng.* **51**(4), 045003 (2012).
23. G. Agrawal, *Nonlinear Fiber Optics*, 3rd ed (Academic Press, 2001).

## 1. Introduction

Fiber optical parametric amplifiers (FOPAs) have attracted much attention over the last two decades and are investigated for many telecommunication applications and ultrafast optical processing technologies in the C and L bands around 1.55  $\mu\text{m}$  [1, 2]. This great interest is motivated by their unique properties such as an extremely wide bandwidth spanning over more than 270 nm [3], a high gain of more than 70 dB [4] and a low noise figure of 3.7 dB [5]. In most of these devices, highly nonlinear fibers (HNLFs) owning a zero-dispersion wavelength (ZDW) around 1.55  $\mu\text{m}$  were used, however the concept of FOPA could be transposed at any other wavelength provided that pump wavelength and fiber properties enable phase matching. In practice, this is not so easy to achieve due to technical limitation imposed by fiber optics components whose performances are usually less optimized than the one devoted to telecommunication applications.

In this work, we focus on the 1  $\mu\text{m}$  spectral region which is of high interest due to the availability of many solid state or ytterbium-doped fiber lasers to which FOPAs could be efficiently associated. FOPAs therefore constitute a promising alternative to usual rare earth-doped fiber amplifiers, as shown recently in the context of fiber optical parametric chirped pulse amplifiers (FOPCPA) [6, 7]. However, quite intriguingly, there has not been any demonstration of continuous-wave (CW) FOPA around 1  $\mu\text{m}$  to date, despite the fact that photonic crystal fibers (PCFs) with a ZDW around 1  $\mu\text{m}$  are now widely available. This is mainly due to the lack of performance of PCFs as compared to HNLFs, the latter having a figure of merit (defined as the ratio of nonlinear coefficient over linear attenuation) about one order of magnitude greater than best PCFs [8]. Other limitations of PCFs include higher splice loss and greater longitudinal dispersion fluctuations with regards to HNLFs. Despite all these drawbacks, pulsed FOPAs have recently been demonstrated at 1  $\mu\text{m}$  [9, 10], by circumventing these limitations thanks to the high peak power available in the pulsed regime. However, the much lower power available for high quality CW lasers makes these limitations crippling for an efficient FOPA.

In this paper, we report a CW FOPA operating around 1  $\mu\text{m}$  in all fiber-integrated format with a record bandwidth of 20 THz. This successful experimental demonstration relies on a PCF with a record figure of merit and strongly reduced longitudinal dispersion fluctuations.

## 2. Fiber properties

The fiber we have used is a PCF with a core highly doped with germanium (Ge). The interest of Ge-doped PCFs has already been demonstrated in the context of Raman lasers [11], CW supercontinuum generation [12] or parametric generation [13] for instance. Basically, doping the core of a PCF with Ge allows for the enhancement of nonlinear Kerr and Raman responses while still keeping the possibility of tailoring the group-velocity dispersion (GVD) curve through a control of the microstructure parameters [14]. In the frame of FOPAs, additional constraints concern the necessity of finely adjusting the ZDW of the PCF in the close vicinity of the available pump wavelength. For this purpose, we kept the same fibre design as the one described in [15] in term of both hole diameter over pitch ratio ( $\sim 0.85$ ) and core Ge doping level ( $\sim 25$  wt %). A pitch value of  $4.0 \mu\text{m}$  allows reaching a ZDW around  $1.05 \mu\text{m}$ . Figure 1(a) shows the GVD curve of the fabricated PCF, calculated with a finite elements method (FEM) from the scanning electron microscope (SEM) image displayed in inset. The ZDW is  $1054 \text{ nm}$  for the neutral axis used in this study. The group birefringence was measured as  $2 \times 10^{-4}$  at  $1064 \text{ nm}$ . The measured attenuation spectrum ( $\alpha$ ) is displayed in Fig. 1(b). At  $1.06 \mu\text{m}$ ,  $\alpha$  and  $\gamma$ , the nonlinear coefficient calculated as in [8], are respectively of  $3.9 \text{ dB/km}$  and  $34 \text{ W}^{-1} \cdot \text{km}^{-1}$ , leading to a twofold improvement of the figure of merit (of  $38 \text{ W}^{-1}$ ) as compared to the recently reported highest value at  $1.06 \mu\text{m}$  [8].

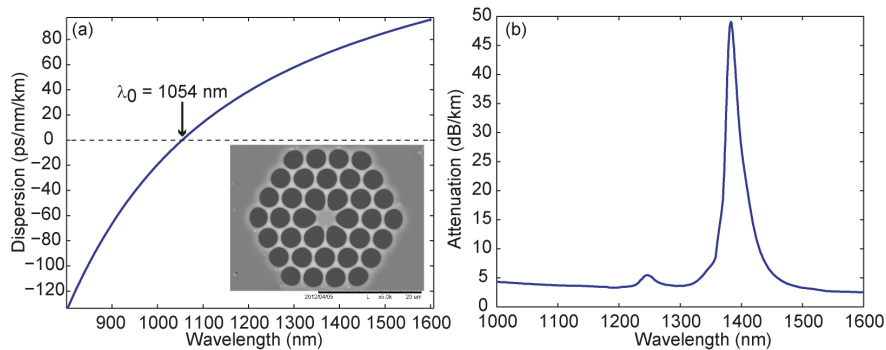


Fig. 1. (a) Calculated GVD curve of the neutral axis used in experiments. Inset: SEM image of the PCF. (b) Measured attenuation spectrum.

Another important parameter that strongly impacts the FOPA performances concerns the stability of dispersion properties along the fiber [16–20], as it directly affects the phase-matching condition. Two contributions to dispersion deviations dominate: a slight continuous drift (due to preform inhomogeneities) and fluctuations around its mean value. In order to minimize the drift, the final preform diameter has been increased as much as possible, leading to a consumption of only  $\sim 10 \text{ mm}$  of preform length to obtain a  $100 \text{ m}$  fiber sample. In order to reduce fluctuations around the mean value, we paid particular attention to choose a particular set of drawing parameters (preform feed rate and argon flow inside the furnace). This allowed reaching a reduced standard deviation of  $0.35 \mu\text{m}$  for an outer diameter of  $158 \mu\text{m}$ . By using FEM computations taking into account only scale modifications of the PCF cross-section, we found that possible variations of the ZDW are about  $\pm 1 \text{ nm}$  along the  $220 \text{ m}$  long fibre sample used for FOPA experiments below.

## 3. Experimental setup

The experimental setup is depicted in Fig. 2. A tunable CW laser (TL-P) is phase modulated by a pseudo random bit sequence at  $3 \text{ GHz}$  in order to mitigate stimulated Brillouin scattering. The output is then amplified by a double-stage ytterbium-doped fiber amplifier with a saturation output power of  $2 \text{ W}$ . The excess of amplified spontaneous emission (ASE) is removed by using a tunable filter of  $1 \text{ nm}$  bandwidth at  $3 \text{ dB}$ . The pump laser is finally

launched together with a second tunable laser (TL-S, the signal) in a 99/1 coupler. All fiber components are polarisation maintaining until the coupler output (labelled A in Fig. 2), which ensures that the pump and the signal polarisation states remain linear. The output port of the coupler is spliced to a single-mode fiber (Hi1060) and the polarisation state of the pump and signal are aligned along one neutral axis of the PCF by using a polarisation controller before being launched into the PCF, where the amplification process takes place. In order to reduce splice losses between the single-mode fiber and the PCF, we insert a small piece of ultra-high numerical aperture (UHNA) fiber that allows for a better mode matching with the PCF. The output average power is 488 mW which corresponds to a power of 670 mW injected inside the PCF. Finally, output spectra are recorded with an optical spectrum analyser (OSA).

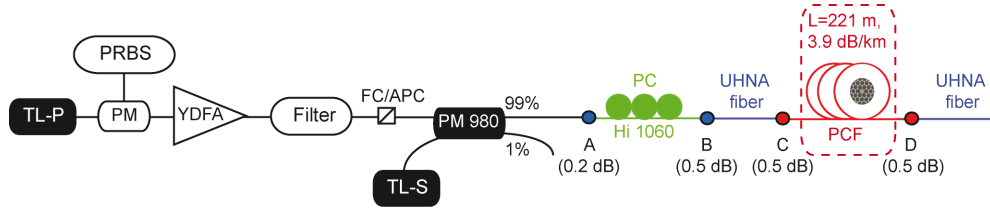


Fig. 2. Experimental setup. TL-P,S: tunable diode lasers, PM: Phase modulator, PRBS: pseudo-random bit sequence, YDFA: Ytterbium doped fiber amplifier, PC: polarization controller.

### 3. Experimental results

Parametric fluorescence or modulation instability spectra were recorded as a function of pump wavelength around the ZDW, without any input signal (TL-S off). They are depicted in Fig. 3, for pump wavelengths ranging from 1054 nm to 1057 nm. As expected, pumping in the normal dispersion region (blue curve in Fig. 3) does not produce any significant parametric fluorescence. Note that the side lobe at 1100 nm is due to stimulated Raman scattering. By moving the pump on the other side of the ZDW, broadband parametric ASE spectra are generated with spectral widths that shrink when increasing the pump wavelength. When the pump wavelength is located just above the ZDW, fluorescence spectra are asymmetric. This can be due to the Raman effect [21, 22], which contribution is reinforced by the strong GeO<sub>2</sub> doping level of this PCF and by the fact that broad parametric gain bands strongly overlap with the Raman one. For pump wavelengths higher than 1054.7 nm, the maxima of the fluorescence signal remain almost constant (less than 2 dB variations on the Stokes side), which means that the parametric process can be considered as insensitive to ZDW longitudinal fluctuations [16].

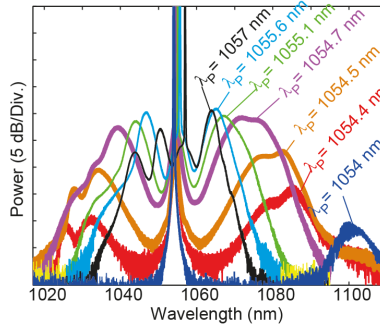


Fig. 3. Parametric fluorescence spectra recorded for increasing pump wavelengths.

This suggests that this PCF exhibits very low ZDW fluctuations as will be discussed hereafter.

Parametric gain spectra were then measured by turning on the input signal and for pump wavelengths of 1054.7 nm and 1054.5 nm (purple and orange bold lines in Fig. 3) corresponding to best compromises between amplification gain and bandwidth. We measured the on/off gain as it is illustrated in Fig. 4(a). Note that the optical noise figure corresponding to this signal was estimated at 15 dB. It is relatively important and it should be due to a quite low optical signal to noise ratio of the pump and to a slight saturation of the amplifier [1]. This will be investigated in details in a future work.

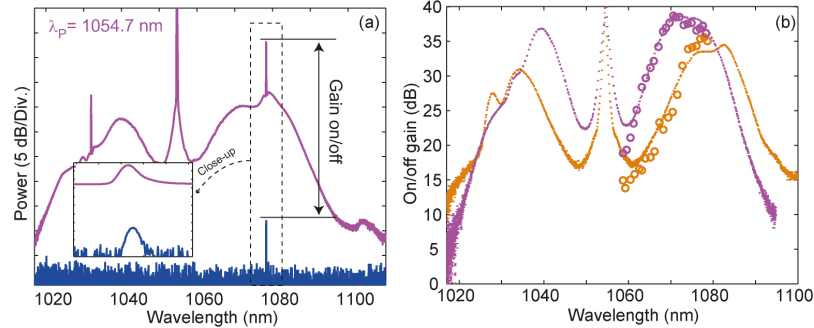


Fig. 4. (a) Output spectra corresponding to pump on (purple line,  $\lambda_p = 1054.7$  nm) and pump off (blue line) when a monochromatic signal is launched into the FOPA. (b) Circles: on/off gain spectra corresponding to  $\lambda_p = 1054.7$  nm (purple) and  $\lambda_p = 1054.5$  nm (orange). Dotted lines represent corresponding parametric fluorescence spectra recorded without any signal. The signal input power was fixed at 740 nW in order to work in the linear regime of the amplifier.

We then measured the on/off gain curves by tuning the signal wavelength. Experimental results are represented in purple and orange circles in Fig. 4(b) for two pump wavelengths, respectively. Unfortunately, our signal tuning range was limited from 1060 nm to 1080 nm and we were therefore unable to record the full gain spectra. In order to get an insight of the whole gain band, we superimposed the parametric fluorescence spectra in dotted lines. A good agreement is achieved on the spectral range where the gain was measured, so we can infer that fluorescence spectra give a good insight of what parametric gain bands should be. A gain of nearly 40 dB at maximum is measured with a pump wavelength of 1054.7 nm and the whole parametric gain band spans over more 20 THz (purple curve). The bandwidth can be slightly increased beyond 20 THz (orange curve) by slightly reducing the pump wavelength from 0.3 nm, which still provides an important maximum gain of 35 dB. It is important to point out that these bandwidths as well as these gain values are of the same order than the best results published to date in FOPAs operating around 1.55  $\mu\text{m}$  [3]. However, our present results were obtained by using a pump power of nearly one order of magnitude lower than the one used in the work of Ref [3].

#### 4. Numerical simulations: impact of longitudinal dispersion fluctuations

Our numerical simulations are performed by integrating the generalized nonlinear Schrödinger equation including the second, third and fourth order dispersion coefficients, and the Raman effect [23]. Dispersion fluctuations have been simulated assuming a Gaussian stochastic process defined by a coherence length and a standard deviation, as in Refs [17, 18]. The standard deviation of the GVD parameter has been deduced from the longitudinal fluctuations of the diameter of the fiber and is  $3 \times 10^{-29}$   $\text{s}^2/\text{m}$ . The coherence length was fixed at 20 m, well above the short scale fluctuations (since they do not impact on parametric processes) and in the order of long scale ones [17, 18]. Finally, as dispersion fluctuations are relatively small, we assumed that the dispersion slope and curvature remain constant on this range of variations. We then calculated 100 gain spectra with random GVD variations. For the sake of clarity, we summarize these results in Fig. 5 as a blue area that corresponds to an

interval of confidence of 68% of the events. The gain curve calculated without ZDW fluctuations is superimposed in black dashed line as a reference. As expected, we see that parametric gain bandwidth can be strongly distorted and lowered by these longitudinal fluctuations. The experimental parametric fluorescence curve, which is assumed to follow the gain curve (see Fig. 4(b)), is superimposed on this figure (orange line). It is located mainly inside the interval of confidence, confirming that our assumptions concerning the reduced fluctuation amplitude of the dispersion are pretty good.

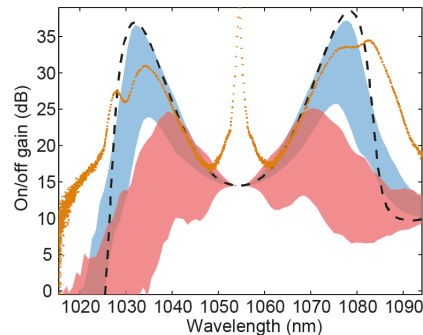


Fig. 5. On/off gain spectra calculated from numerical simulations, without dispersion fluctuation (black dashed line), blue band with reduced ZDW fluctuations and red band with standard ones with an interval of confidence of 68% of the events. Experimental results with  $\lambda_p = 1054.5$  nm are represented in orange line. Parameters are similar to experimental ones.  $\lambda_p = 1054.5$  nm,  $\beta_2(\lambda_p)$  average  $= -1 \times 10^{-29}$  s<sup>2</sup>/m,  $\beta_3(\lambda_p) = 0.56 \times 10^{-40}$  s<sup>3</sup>/m,  $\beta_4(\lambda_p) = -1.5 \times 10^{-55}$  s<sup>4</sup>/m,  $\gamma = 35$  W<sup>-1</sup>.km<sup>-1</sup>,  $L = 220$  m,  $P_p = 670$  mW and  $\alpha = 3.9$  dB/km.

In order to highlight the crucial importance of lowering longitudinal dispersion fluctuations, we performed additional simulations with a standard deviation 3 times larger. This value corresponds to the standard value we have in our drawing tower when no special care is paid to stabilize the drawing process. The results are represented in a red band in Fig. 5. The maximum gain value would be about 10 dB lower and the spectral bandwidth about two times less broad. It really highlights that the success of this experiment is based on the high quality of the fiber we fabricated and explains why it was impossible to succeed with a fiber with a lower figure of merit and with relatively significant longitudinal fluctuations [9, 10].

## 5. Conclusion

We have reported the experimental demonstration of the first CW all-fiber optical parametric amplifier operating around 1  $\mu$ m, based on a dispersion-stabilized Ge-doped highly nonlinear PCF with a record figure of merit. This PCF has been specially designed to allow for the achievement of a broadband FOPA at 1  $\mu$ m with a maximum gain approaching 40 dB and a bandwidth spanning over more than 20 THz. These performances are comparable to the best ones reported around 1.55  $\mu$ m, but with a pump power nearly one order of magnitude lower. FOPAs operating near 1  $\mu$ m could be combined to widely spread solid state or ytterbium-doped fiber lasers emitting in this spectral region. They should provide an interesting alternative to ytterbium-doped fiber amplifiers in view of potential applications to ultrafast signal processing such as ultrafast optical gating and chirped-pulse amplification at 1  $\mu$ m.

## Acknowledgments

We acknowledge Armand Vedadi for fruitful discussions. This work was partly supported by the Agence Nationale de la Recherche through the ANR FOPAFE project, by the French Ministry of Higher Education and Research, the Nord-Pas de Calais Regional Council and Fonds Européen de Développement Régional through the “Contrat de Projets Etat Région (CPER) 2007-2013” and the “Campus Intelligence Ambiante (CIA)”.